



Estimation of fractured weaknesses and attenuation factors from azimuthal seismic data

Huaizhen Chen and Kris Innanen

CREWES project, Department of Geoscience, University of Calgary

Summary

Seismic wave propagation in fractured reservoirs exhibits anisotropy and attenuation that are related to fracture properties (e.g. fracture density) and fluid parameters (e.g., fluid moduli and viscosity). Based on the linear slip theory, we derive stiffness parameters for fractured and attenuative rocks, and present the integrated attenuation factors involving both host rock intrinsic attenuation and fracture-induced attenuation. Using the simplified stiffness parameters, we derive a linearized reflection coefficient in terms of fracture weaknesses and integrated attenuation factors. A two-step inversion approach is proposed, which involves an iterative damped least-squares algorithm to predict P- and S-wave moduli using angle gathers at the azimuthal angle approximately equal to fracture orientation azimuth, and a Bayesian inversion method to estimate fracture weaknesses and integrated attenuation factors from seismic amplitude differences among the data at different azimuthal angles. The proposed approach is testified on a real data set, within which we observe that reasonable parameters (fracture weaknesses and integrated attenuation factors) are determined.

Introduction

The linear slip theory describes the effect of fractures on elastic parameters using fracture weaknesses or compliances (Schoenberg and Sayers, 1995). Bakulin et al. (2000) related the normal and tangential fracture weaknesses to fracture properties (fracture density, fracture aspect ratio and fillings). Chen et al. (2017) studied how the normal and tangential fracture weaknesses change in the case of water and oil saturated rocks, which shows that the normal fracture weakness difference between water and oil fractured rocks is relatively small. It indicates that the normal fracture weakness is not a sensitive indicator to discriminate water and oil saturated fractures. Hence, in the present study, we will involve the attenuation factor as an additional factor for fluid identification. Much work has been done to study how the attenuation affects the rock property and seismic wave propagation. Hudson et al. (1996) studied the effect of connection between cracks and pores on the overall property of a cracked rock. Pointer et al. (2000) discussed how the distribution and saturation of cracks affect the response quantity. Based on the linear slip theory, Chichinina et al. (2006) proposed the complex normal and tangential fracture weaknesses that related to Q anisotropy. Chen et al. (2017) proposed to use amplitude differences among azimuthal data to implement seismic inversion, which can lead to a stable estimation of the normal and tangential fracture weaknesses. In this study, we first express perturbations in the simplified stiffness parameters in the case of an interface separating two anisotropic and attenuative media. Using the perturbations, we then derive a linearized reflection coefficient as a function of integrated attenuation factors and fracture weaknesses. We finally propose an inversion method to estimate integrated attenuation factors and fracture weaknesses from azimuthal seismic data. A test on real data acquired over a fractured reservoir demonstrates that the proposed approach can estimate reasonable parameters for fracture prediction and fluid discrimination.

Linearized PP- wave reflection coefficient

Involving effects of both background and fracture-induced attenuation, we propose the complex stiffness matrix

$$\bar{\mathbf{C}} = \begin{bmatrix} \bar{M}(1-\bar{\Delta}_N) & \bar{\lambda}(1-\bar{\Delta}_N) & \bar{\lambda}(1-\bar{\Delta}_N) & 0 & 0 & 0 \\ \bar{\lambda}(1-\bar{\Delta}_N) & \bar{M}(1-\bar{\chi}^2\bar{\Delta}_N) & \bar{\lambda}(1-\bar{\chi}\bar{\Delta}_N) & 0 & 0 & 0 \\ \bar{\lambda}(1-\bar{\Delta}_N) & \bar{\lambda}(1-\bar{\chi}\bar{\Delta}_N) & \bar{M}(1-\bar{\chi}^2\bar{\Delta}_N) & 0 & 0 & 0 \\ 0 & 0 & 0 & \bar{\mu} & 0 & 0 \\ 0 & 0 & 0 & 0 & \bar{\mu}(1-\bar{\Delta}_T) & 0 \\ 0 & 0 & 0 & 0 & 0 & \bar{\mu}(1-\bar{\Delta}_T) \end{bmatrix}, \quad (1)$$

where

$$\bar{M} \approx M(1+i/Q_P), \bar{\mu} \approx \mu(1+i/Q_S), \bar{\Delta}_N = \Delta_N - i(1-\Delta_N)/Q_N, \bar{\Delta}_T = \Delta_T - i(1-\Delta_T)/Q_T, \quad (2)$$

and where Δ_N and Δ_T represent the real parts of fracture weaknesses, $1/Q_N$ and $1/Q_T$ are parameters related to fracture-induced attenuation, $1/Q_P$ and $1/Q_S$ are P- and S-wave attenuation factors while propagating in the isotropic and attenuative background, $M = \lambda + 2\mu$, $\chi = \lambda/M = 1 - 2g$, and λ and μ are Lamé constants of the elastic and isotropic background.

We express perturbations in stiffness parameters for the case of a reflection interface separating two fractured and attenuative layers. In the present study, we focus on the derivation of the real part of P-to-P reflection coefficient. The real parts of perturbations in the complex stiffness parameters are given by

$$\begin{aligned} \Delta C_{11} &\approx \Delta M - \Delta M/Q_{PN} - M\Delta(1/Q_{PN}) - M\delta_{\Delta_N}, \\ \Delta C_{12} &\approx \Delta\lambda - \lambda\delta_{\Delta_N} - \Delta M/Q_{PN} - M\Delta(1/Q_{PN}) + 2\Delta\mu/Q_{SN} + 2\mu\Delta(1/Q_{SN}), \\ \Delta C_{23} &\approx \Delta\lambda + (2g-1)\lambda\delta_{\Delta_N} + (2g-1)\Delta M/Q_{PN} + (2g-1)M\Delta(1/Q_{PN}) + (2-4g)\Delta\mu/Q_{SN} + (2-4g)\mu\Delta(1/Q_{SN}), \quad (3) \\ \Delta C_{33} &\approx \Delta M - M\delta_{\Delta_N} + 4Mg(1-g)\delta_{\Delta_N} + 4g(1-g)\Delta M/Q_{PN} + 4g(1-g)M\Delta(1/Q_{PN}), \\ \Delta C_{44} &= \Delta\mu, \Delta C_{55} \approx \Delta\mu - \Delta\mu/Q_{ST} - \mu\Delta(1/Q_{ST}) - \mu\delta_{\Delta_T}, \end{aligned}$$

where ΔM is perturbation in the compressional modulus across the interface, $\Delta\lambda$ and $\Delta\mu$ are changes in Lamé constants across the interface, δ_{Δ_N} and δ_{Δ_T} are changes in the normal and tangential fracture weaknesses across the interface, $1/Q_{PN} = 1/(Q_P Q_N)$, $1/Q_{SN} = 1/(Q_S Q_N)$, $1/Q_{ST} = 1/(Q_S Q_T)$, $\Delta(1/Q_{PN})$, $\Delta(1/Q_{SN})$ and $\Delta(1/Q_{ST})$ are changes in the corresponding inverse quality factors. Shaw and Sen (2004) proposed a method to use the scattering function involving perturbation in stiffness matrix to derive linearized reflection coefficients. Following Shaw and Sen (2004), we derive the linearized P-to-P complex reflection coefficient as

$$\begin{aligned} R_{pp}(\theta, \phi) &= P_M(\theta)\Delta M/M + P_\mu(\theta)\Delta\mu/\mu + P_\rho(\theta)\Delta\rho/\rho, \\ &+ P_{Q_{PN}}(\theta, \phi)\Delta(1/Q_{PN}) + P_{Q_{SN}}(\theta, \phi)\Delta(1/Q_{SN}) + P_{\Delta_N}(\theta, \phi)\delta_{\Delta_N} + P_{\Delta_T}(\theta, \phi)\delta_{\Delta_T}, \end{aligned} \quad (4)$$

where $P_M(\theta) = 1/4\sec^2\theta$, $P_\mu(\theta, g) = -2g\sin^2\theta$, $P_\rho(\theta) = \cos 2\theta/(4\cos^2\theta)$,

$$P_{Q_{PN}}(\theta, \phi, g) = \frac{1}{4}\sec^2\theta \left[-\sin^4\theta \cos^2\phi(1+\sin^2\phi) + 2\sin^2\theta \cos^2\theta(2g\sin^2\phi-1) + 4g(1-g)(\sin^4\theta \sin^4\phi + \cos^4\theta) \right],$$

$P_{Q_{SN}}(\theta, \phi, g) = g \sin^2 \theta (\tan^2 \theta \sin^2 \phi \cos^2 \phi + 1 - 2g \sin^2 \phi)$, $P_{\Delta_N}(\theta, \phi, g) = -\frac{1}{4} \sec^2 \theta [1 - 2g (\sin^2 \theta \sin^2 \phi + \cos^2 \theta)]^2$,
 $P_{\Delta_T}(\theta, \phi, g) = g \sin^2 \theta \cos^2 \phi (1 - \tan^2 \theta \sin^2 \phi)$, and where $\Delta M/M$, $\Delta \mu/\mu$, and c are relative changes in P-wave modulus, S-wave modulus, and density across the interface, and δ_{Δ_N} and δ_{Δ_T} are changes in the normal and tangential fracture weaknesses across the interface.

Estimation of integrated inverse quality factors from seismic data

We employ seismic amplitude differences among the input data at different azimuthal angles to estimate the integrated inverse quality factors and fracture weaknesses. The seismic amplitude differences in the case of five azimuthal angles (i.e. $\phi_1, \phi_2, \phi_3, \phi_4$ and ϕ_5) are given by

$$\mathbf{B} = \mathbf{A}\mathbf{X}, \quad (5)$$

where

$$\mathbf{B} = \begin{bmatrix} s(\phi_2) - s(\phi_1) \\ s(\phi_3) - s(\phi_1) \\ s(\phi_4) - s(\phi_1) \\ s(\phi_5) - s(\phi_1) \end{bmatrix}, \quad \mathbf{X} = \begin{bmatrix} R_{Q_{PN}} \\ R_{Q_{SN}} \\ R_{\Delta_N} \\ R_{\Delta_T} \end{bmatrix},$$

$$\mathbf{A} = \mathbf{W} \begin{bmatrix} P_{Q_{PN}}(\phi_2) - P_{Q_{PN}}(\phi_1) & P_{Q_{SN}}(\phi_2) - P_{Q_{SN}}(\phi_1) & P_{\Delta_N}(\phi_2) - P_{\Delta_N}(\phi_1) & P_{\Delta_T}(\phi_2) - P_{\Delta_T}(\phi_1) \\ P_{Q_{PN}}(\phi_3) - P_{Q_{PN}}(\phi_1) & P_{Q_{SN}}(\phi_3) - P_{Q_{SN}}(\phi_1) & P_{\Delta_N}(\phi_3) - P_{\Delta_N}(\phi_1) & P_{\Delta_T}(\phi_3) - P_{\Delta_T}(\phi_1) \\ P_{Q_{PN}}(\phi_4) - P_{Q_{PN}}(\phi_1) & P_{Q_{SN}}(\phi_4) - P_{Q_{SN}}(\phi_1) & P_{\Delta_N}(\phi_4) - P_{\Delta_N}(\phi_1) & P_{\Delta_T}(\phi_4) - P_{\Delta_T}(\phi_1) \\ P_{Q_{PN}}(\phi_5) - P_{Q_{PN}}(\phi_1) & P_{Q_{SN}}(\phi_5) - P_{Q_{SN}}(\phi_1) & P_{\Delta_N}(\phi_5) - P_{\Delta_N}(\phi_1) & P_{\Delta_T}(\phi_5) - P_{\Delta_T}(\phi_1) \end{bmatrix}, \quad (6)$$

and where s is the vector of observed seismic data, and \mathbf{W} is the vector of seismic wavelet.

In order to solve the inverse problem, we employ the Bayesian theorem to construct the objective function. Assuming uniform uncorrelated Gaussian noise included in observed seismic data and given a prior information satisfying Cauchy distribution, we present the objective function

$$J(\mathbf{X}) = (\mathbf{B} - \mathbf{A}\mathbf{X})^T (\mathbf{B} - \mathbf{A}\mathbf{X}) / (2\sigma_{\text{noise}}^2) + \ln [1 + \mathbf{X}^2 / (2\sigma_{\mathbf{X}}^2)]. \quad (7)$$

We employ an iterative approach to obtain the inversion result

$$\mathbf{X}_{i+1} = \mathbf{X}_i + \left[\mathbf{A}^T \mathbf{A} + 4\sigma_{\text{noise}}^2 / (1 + 0.5\mathbf{X}_i^2 / \sigma_{\mathbf{X}_i}^2) \right]^{-1} \mathbf{A}^T (\mathbf{B} - \mathbf{A}\mathbf{X}_i), \quad (8)$$

where \mathbf{X}_{i+1} is the calculated result based on the i th solution \mathbf{X}_i , and \mathbf{X}_1 is the initial solution of the unknown parameter vector.

Examples

We utilize a real dataset acquired over a fractured carbonate rock reservoir, which is respectively processed in offset and azimuth domains, to verify the proposed inversion approach. We first use the data along the fracture orientation azimuth to estimate P- and S-wave moduli (Figure1).

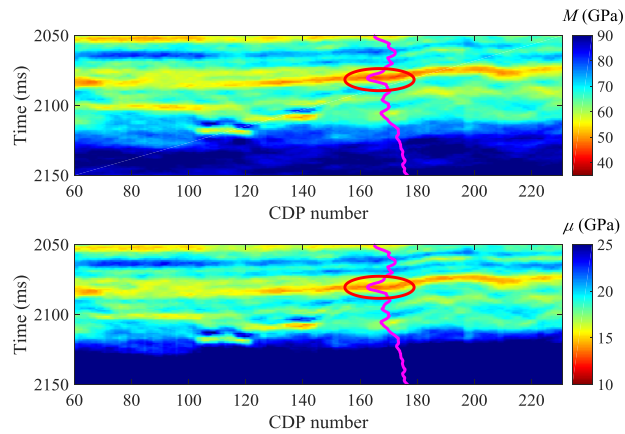


Figure 1. Inversion results of P- and S-wave moduli. The ellipse indicates the fracture reservoir.

Using the Bayesian inversion as presented in the previous section, we implement the iterative inversion for the integrated inverse quality factors and fracture weaknesses (Figure 2). we observe that there is a good match between P-wave velocity curve and the inversion result.

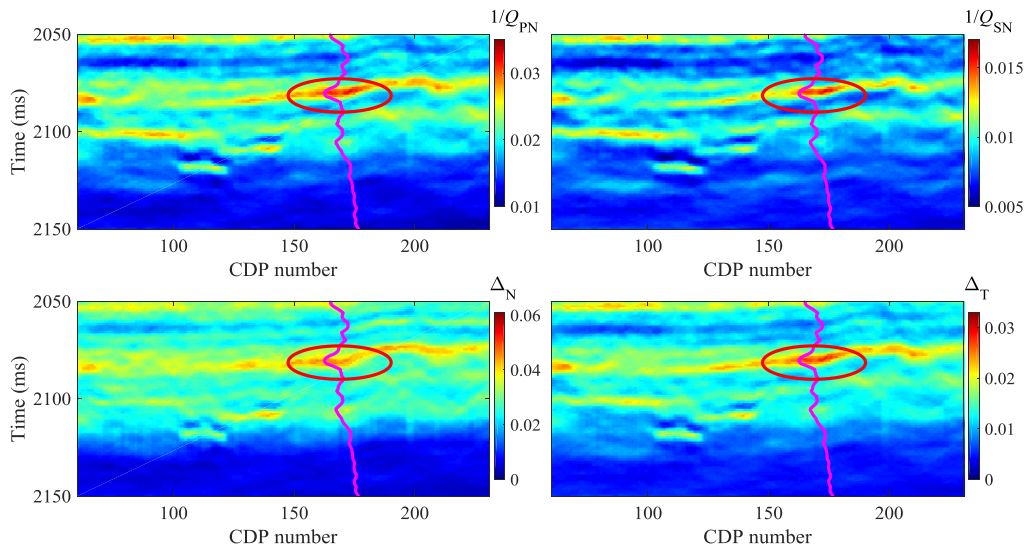


Figure 2. Inversion results of integrated attenuation factors and fracture weaknesses.

Conclusions

We begin with the derivation of perturbations in stiffness parameters for the case of an interface separating two fractured and attenuative media. Using the perturbations, we derive a linearized reflection coefficient in terms of P- and S-wave moduli, integrated attenuation factors and fracture weaknesses. Based on the derived reflection coefficient, we propose an inversion method to use azimuthal seismic data to estimate fracture weaknesses and integrated attenuation factors. Applying the proposed inversion method to a real data set reveals that the proposed inversion method can provide realistic results of integrated attenuation factors and fracture weaknesses for fracture prediction and fluid discrimination.

Acknowledgements

The industrial sponsors of CREWES are thanked for their support. We gratefully acknowledge support from NSERC through the grant CRDPJ 461179-13. This research was undertaken thanks in part to funding from the Canada First Research Excellence Fund and Mitacs Project. The SINOPEC is thanked for providing the data.

References

- Bakulin, A., Grechka, V., and Tsvankin, I., 2000, Estimation of fracture parameters from reflection seismic data—Part I: HTI model due to a single fracture set: *Geophysics*, 65, No. 6, 1788–1802.
- Chen, H., Zhang, G., Ji, Y., and Yin, X., 2017, Azimuthal seismic amplitude difference inversion for fracture weakness: *Pure and Applied Geophysics*, 174, No. 1, 279–291.
- Chichinina, T., Sabinin, V., and Ronquillo-Jarillo, G., 2006, QVOA analysis: P-wave attenuation anisotropy for fracture characterization: *Geophysics*, 71, No. 3, C37–C48.
- Hudson, J., Liu, E., and Crampin, S., 1996, The mechanical properties of materials with interconnected cracks and pores: *Geophysical Journal International*, 124, No. 1, 105–112.
- Pointer, T., Liu, E., and Hudson, J. A., 2000, Seismic wave propagation in cracked porous media: *Geophysical Journal International*, 142, No. 1, 199–231.
- Schoenberg, M., and Sayers, C. M., 1995, Seismic anisotropy of fractured rock: *Geophysics*, 60, No. 1, 204–211.
- Shaw, R. K., and Sen, M. K., 2004, Born integral, stationary phase and linearized reflection coefficients in weak anisotropic media: *Geophysical Journal International*, 158, No. 1, 225–238.